

Thermally-Induced Acid Generation from 18-Molybdodiphosphate and 18-Tungstodiphosphate within Poly(2-Hydroxyethyl Methacrylate) Films

Antonios M. Douvas,^{*,†} Konstantina Yannakopoulou,[‡] and Panagiotis Argitis^{*,†}

[†]Institute of Microelectronics and [‡]Institute of Physical Chemistry, National Center for Scientific Research “Demokritos”, 15310 Aghia Paraskevi, Athens, Greece

Received October 2, 2009. Revised Manuscript Received March 18, 2010

The thermally induced acid generation by two Dawson-type polyoxometalates (POMs), namely, the ammonium 18-molybdodiphosphate, $(\text{NH}_4)_6\text{P}_2\text{Mo}_{18}\text{O}_{62}$, (Mo_{18}^{6-}) and the ammonium 18-tungstodiphosphate, $(\text{NH}_4)_6\text{P}_2\text{W}_{18}\text{O}_{62}$, (W_{18}^{6-}) within poly(2-hydroxyethyl methacrylate) (PHEMA) films is reported. The acid is generated by the simultaneous thermal reduction of POMs and oxidation of a small percentage of PHEMA hydroxyl groups, and it subsequently catalyzes the cross-linking of the polymer. The generated protons are detected by introducing a known acid indicator (methylene blue, MB) within the films and monitoring the indicator's protonation with UV spectroscopy. The acid-catalyzed cross-linking of PHEMA is studied by dissolution studies supported with FTIR and NMR spectroscopy. From the combination of those two spectroscopic studies it is concluded that PHEMA cross-linking within POM-PHEMA films is an acid-catalyzed reaction involving elimination of hydroxyl groups (possibly transesterification) accompanied by the side reaction of acid-catalyzed dehydration of PHEMA that leads to the formation of soluble products. Both POMs investigated can be completely removed, if desired, from the thermally cross-linked PHEMA films at the end of the process, by incubation in an aqueous solution of base, allowing therefore the use of POMs as acid generating agents in applications where the removal of the acid generator from the polymer films is beneficial.

Introduction

During the past few years a significant increase in the research activity regarding polyoxometalates (POMs) is observed, mostly because of the high industrial and academic interest in those compounds.¹ That trend has been considerably supported by the synthesis of new, more advanced POM structures,² the improvement in their characterization methods, and the contemporary theoretical investigations of POMs,³ as they contributed to the deeper understanding of their structure, electronic properties, and chemical reactivity.⁴ In general, POMs are metal–oxygen anionic clusters with well-defined molecular structure,⁵ which are well-known for, among others, the following properties: (a) they can thermally or photochemically oxidize a vast number of organic

compounds, because of their capability to accept a certain number of electrons without substantial change of their structure;^{6–8} and (b) they are very weak Brønsted bases, and thus their conjugate acids (the heteropoly acids) are very strong Brønsted acids with an acidity approaching the super acids' region.^{9,10} Because of those two fundamental properties, POMs are used in a broad field of applications in both oxidation and acid catalysis,^{6,9,11} and recently have been considered in additional applications as well, such as fuel cells,¹² molecular conductors,¹³ proton memory devices,¹⁴ and solid-state electronic devices.¹⁵

*To whom correspondence should be addressed. E-mail: adouvas@imel.demokritos.gr (A.M.D.), argitis@imel.demokritos.gr (P.A.). Fax: +30-210-6511723. Phone: +30-210-6503231 (A.M.D.), +30-210-6503114 (P.A.).

- (1) (a) Long, D.-L.; Tsunashima, R.; Cronin, L. *Angew. Chem., Int. Ed.* **2010**, *49*, 2. (b) Long, D.-L.; Burkholder, E.; Cronin, L. *Chem. Soc. Rev.* **2007**, *36*, 105.
- (2) (a) Müller, A.; Roy, S. *Coord. Chem. Rev.* **2003**, *245*, 153. (b) Müller, A.; Beckmann, E.; Bögge, H.; Schmidtmann, M.; Dress, A. *Angew. Chem., Int. Ed.* **2002**, *41*, 1162.
- (3) (a) Poblet, J. M.; López, X.; Bo, C. *Chem. Soc. Rev.* **2003**, *32*, 297. (b) López, X.; Bo, C.; Poblet, J. M. *J. Am. Chem. Soc.* **2002**, *124*, 12574.
- (4) (a) Mizuno, N.; Yamaguchi, K.; Kamata, K. *Coord. Chem. Rev.* **2005**, *249*, 1944. (b) Geletii, Y. V.; Botar, B.; Kögerler, P.; Hillesheim, D. A.; Musaev, D. G.; Hill, C. L. *Angew. Chem., Int. Ed.* **2008**, *47*, 3896.
- (5) (a) Pope, M. T.; Müller, A. *Angew. Chem., Int. Ed. Engl.* **1991**, *30*, 34. (b) Pope, M. T. *Heteropoly and Isopoly Oxometalates*; Springer-Verlag: Berlin, 1983.
- (6) Misono, M.; Nojiri, N. *Appl. Catal.* **1990**, *64*, 1.
- (7) Papaconstantinou, E. *Chem. Soc. Rev.* **1989**, *18*, 1.
- (8) Hiskia, A.; Mylonas, A.; Papaconstantinou, E. *Chem. Soc. Rev.* **2001**, *30*, 62.
- (9) Kozhevnikov, I. V. *Chem. Rev.* **1998**, *98*, 171.
- (10) Drago, R. S.; Dias, J. A.; Maier, T. O. *J. Am. Chem. Soc.* **1997**, *119*, 7702.
- (11) (a) Matveev, K. I.; Odyakov, V. F.; Zhizhina, E. G. *J. Mol. Catal. A* **1996**, *114*, 151. (b) Neumann, R.; Kenkin, A. M. *J. Mol. Catal. A* **1996**, *114*, 169.
- (12) Kim, W. B.; Voigt, T.; Rodriguez-Rivera, G. J.; Dumesic, J. A. *Science* **2004**, *305*, 1280.
- (13) Coronado, E.; Giménez-Saiz, C.; Gómez-García, C. J. *Coord. Chem. Rev.* **2005**, *249*, 1776.
- (14) (a) Kapetanakis, E.; Douvas, A. M.; Velessiotis, D.; Makarona, E.; Argitis, P.; Glezos, N.; Normand, P. *Adv. Mater.* **2008**, *20*, 4568. (b) Kapetanakis, E.; Douvas, A. M.; Velessiotis, D.; Makarona, E.; Argitis, P.; Glezos, N.; Normand, P. *Org. Electron.* **2009**, *10*, 711.
- (15) (a) Douvas, A. M.; Makarona, E.; Glezos, N.; Argitis, P.; Mielczarski, J. A.; Mielczarski, E. *ACS Nano* **2008**, *2*, 733. (b) Makarona, E.; Kapetanakis, E.; Velessiotis, D. M.; Douvas, A.; Argitis, P.; Normand, P.; Gotszalk, T.; Woszczyna, M.; Glezos, N. *Microelectron. Eng.* **2008**, *85*, 1399. (c) Glezos, N.; Argitis, P.; Velessiotis, D.; Diakoumakos, C. D. *Appl. Phys. Lett.* **2003**, *83*, 488.

The photooxidizing behavior of POMs has been extensively studied, mainly in solutions in the presence of organic substrates.^{7,8,16} In contrast, a relatively limited number of studies about this issue has been performed within polymer films. A characteristic example is the photoreduction of 12-tungstophosphoric acid ($\text{H}_3\text{PW}_{12}\text{O}_{40}$) within poly(vinyl alcohol) (PVA) films, where photooxidation of PVA and subsequent Diels–Alder cross-linking takes place selectively in the exposed film areas.¹⁷ Another study of POMs within polymer films that investigates the combination of both major POM properties (i.e., their photooxidizing efficiency and their low Brønsted basicity) was recently reported by our group.¹⁸ In that paper, the capability of two Dawson-type POMs (namely, the ammonium 18-molybdodiphosphate, $(\text{NH}_4)_6\text{P}_2\text{Mo}_{18}\text{O}_{62}$ (Mo_{18}^{6-}) and the ammonium 18-tungstodiphosphate, $(\text{NH}_4)_6\text{P}_2\text{W}_{18}\text{O}_{62}$ (W_{18}^{6-})) to photochemically generate acid within films of a polymer with hydroxyl functional groups (and in particular PHEMA) was demonstrated, where the generated acid was used for catalyzing cross-linking reactions of the polymer matrix.

In continuation of the latter work, the capability of the same Dawson-type POMs (i.e., the ammonium salts of Mo_{18}^{6-} and W_{18}^{6-}) to thermally generate protons within PHEMA films is investigated in the present paper. Although a significant number of studies have been reported regarding photoacid generators (PAGs), with the most representative being diaryliodonium^{19a,b} and triarylsulfonium salts,^{19c,d} and *o*-nitrobenzyl esters,^{19e} a relatively low number of studies have been devoted to thermal acid generators (TAGs). Nevertheless, TAGs are of significant practical and academic importance, as they find applications as thermal initiators for cationic polymerization,^{20,21} as curing agents in coatings and paints,²² and also in microlithographic applications.²³ The compounds mostly reported as efficient TAGs are, in general, similar to those proposed as PAGs, and they generate acid through an intramolecular thermolysis reaction. The most known TAGs are various sulfonates (such as am-

monium sulfonates, *o*-nitrobenzyl tosylates,²² benzoin tosylates,²⁴ etc), and a range of diaryliodonium^{20a,b} and sulfonium salts.^{20c,d} It should be also noticed that the majority of the known TAGs (especially those used as thermal initiators for cationic polymerization)²¹ thermally yield strong Lewis acids, but in a rather limited number of cases (e.g., the *o*-nitrobenzyl tosylate as a thermal source of *p*-toluenesulfonic acid) they thermally generate protons, which are generally preferred in solid state catalysis.

In the present work, it is shown that protons are generated by the thermal reduction of both Dawson-type POMs and the associated oxidation of PHEMA, following a mechanism similar to the generally accepted mechanism for the photocatalytic oxidation of alcohols by POMs in solution.^{7,25} The thermally generated protons catalyze next the cross-linking of PHEMA. The generated acid within PHEMA films is detected by monitoring the protonation of a suitable acid indicator (methylene blue, MB) with UV spectroscopy. Also, the acid-catalyzed cross-linking of PHEMA is studied by dissolution studies supported with FTIR and NMR spectroscopy. Furthermore, it is shown that both POMs investigated can be entirely removed from the thermally cross-linked POM-PHEMA films by incubating those films in an aqueous solution of base (e.g., tetramethylammonium hydroxide, TMAH 0.26 M), making therefore, those materials attractive for applications that require removal of the acid generator from the films at the end of the process.

Experimental Section

Materials. Two Dawson-type POMs (both α isomers), namely, the ammonium 18-molybdodiphosphate, $\alpha\text{-(NH}_4)_6\text{P}_2\text{Mo}_{18}\text{O}_{62} \cdot x\text{H}_2\text{O}$, (Mo_{18}^{6-}) and the ammonium 18-tungstodiphosphate, $\alpha\text{-(NH}_4)_6\text{P}_2\text{W}_{18}\text{O}_{62} \cdot x\text{H}_2\text{O}$, (W_{18}^{6-}) were prepared according to well-established methods.²⁶ 12-tungstophosphoric acid hydrate $\text{H}_3\text{PW}_{12}\text{O}_{40} \cdot x\text{H}_2\text{O}$ (obtained from Aldrich), triphenylsulfonium hexafluoroantimonate ($\text{Ph}_3\text{S}^+\text{SbF}_6^-$; TPHFA; obtained from Midori Kagakou), and methylene blue hydrate (MB; obtained from Fluka) were of analytical grade and used without further purification. The homopolymer poly(2-hydroxyethyl methacrylate) (PHEMA; MW 300,000; purchased from Aldrich) was used as received. The solvents methanol, ethanol, ethyl lactate (EL), dimethyl sulfoxide (DMSO; obtained from Aldrich), and DMSO-*d*₆ (purchased from Deutero GmbH) were also of analytical grade. The industry-standard aqueous solution of tetramethylammonium hydroxide (TMAH 0.26 M; a developer solution with the trade name AZ 726 MIF) was supplied from Clariant. Deionized water (with a resistivity of 15 M Ω cm⁻¹) prepared from the Milli-RO plus 90 apparatus (Millipore) was used where necessary.

Film Preparation, Characterization, and Curing. Solutions of PHEMA (3.11–6.28 w/w in EL; 4–5% w/w in MeOH; 3.29–4.71% w/w in a MeOH/water mixture at a weight ratio ranging from 1.3:1 to 2.2:1; 2.5% w/w in DMSO) were prepared. In some of the PHEMA solutions, one of the following compounds: Mo_{18}^{6-} (0.11–53.9% w/w in solids), W_{18}^{6-} (0.29–50% w/w

- (16) Chambers, R. C.; Hill, C. L. *Inorg. Chem.* **1991**, *30*, 2776.
- (17) Carls, J. C.; Argitis, P.; Heller, A. J. *Electrochem. Soc.* **1992**, *139*, 786.
- (18) Douvas, A. M.; Kapella, A.; Dimotikali, D.; Argitis, P. *Inorg. Chem.* **2009**, *48*, 4896.
- (19) (a) Crivello, J. V.; Lam, J. H. W. *Macromolecules* **1977**, *10*, 1307. (b) Dektar, J. L.; Hacker, N. P. *J. Org. Chem.* **1990**, *55*, 639. (c) Crivello, J. V.; Lam, J. H. W. *J. Polym. Sci., Part A: Polym. Chem.* **1979**, *17*, 977. (d) Dektar, J. L.; Hacker, N. P. *J. Am. Chem. Soc.* **1990**, *112*, 6004. (e) Houlihan, F. M.; Neenan, T. X.; Reichmanis, E.; Kometani, J. M.; Chin, T. *Chem. Mater.* **1991**, *3*, 462.
- (20) (a) Crivello, J. V.; Lockhart, T. P.; Lee, J. L. *J. Polym. Sci., Part A: Polym. Chem.* **1983**, *21*, 97. (b) Crivello, J. V.; Lee, J. L. *J. Polym. Sci., Part A: Polym. Chem.* **1989**, *27*, 3951. (c) Crivello, J. V.; Lee, J. L. *Polymer J.* **1985**, *17*, 73. (d) Endo, T.; Uno, H. *J. Polym. Sci. Polym. Lett. Ed.* **1985**, *23*, 359.
- (21) (a) Shimomura, O.; Tomita, I.; Endo, T. *J. Polym. Sci., Part A: Polym. Chem.* **2001**, *39*, 3928. (b) Hamazu, F.; Akashi, S.; Koizumi, T.; Takata, T.; Endo, T. *J. Polym. Sci., Part A: Polym. Chem.* **1993**, *31*, 1023. (c) Sundell, P.-E.; Jönsson, S.; Hult, A. *J. Polym. Sci., Part A: Polym. Chem.* **1991**, *29*, 1535.
- (22) Cameron, J. F.; Fréchet, J. M. J. *Polymer Bull.* **1991**, *26*, 297.
- (23) (a) Oberlander, J.; Wanat, S.; McKenzie, D.; Kokinda, E. *Proc. SPIE* **2000**, *3999*, 655. (b) Hwang, S.-H.; Lee, K.-K.; Jung, J.-C. *Polymer* **2000**, *41*, 6691.
- (24) Gatechair, L. R. *Proc. Polym. Mater. Sci. Eng.* **1988**, *59*, 289.

- (25) Papaconstantinou, E.; Ioannidis, A.; Hiskia, A.; Argitis, P.; Dimotikali, D.; Korres, S. *Mol. Eng.* **1993**, *3*, 231.
- (26) Wu, H. *J. Biol. Chem.* **1920**, *43*, 189.

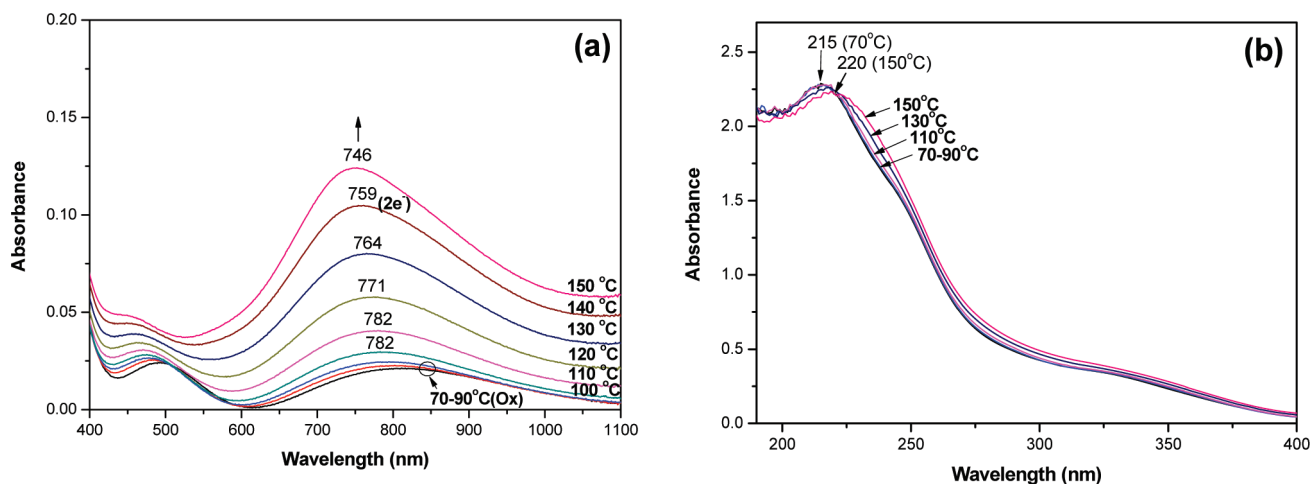


Figure 1. UV monitoring of the thermal reduction of the Mo_{18}^{6-} ions within PHEMA films, in the temperature range of 70 to 150 °C: (a) change of the IVCT band, and (b) change of the OMCT band of the Mo_{18}^{6-} ions. The thermal treatment temperatures (°C) and the positions (nm) of both IVCT and OMCT bands of the Mo_{18}^{6-} ions are indicated on spectra. (Solution Mo_{18}^{6-} -PHEMA, 53.4–6.28% (w/w EL). Thermal treatment time, 5 min. Initial film thickness, 256 nm.).

in solids), TPSHFA (23.1% w/w in solids), or $\text{H}_3\text{PW}_{12}\text{O}_{40}$ (0.12–63.5% w/w in solids) was added. In some of the resulted solutions, MB (at a molar ratio of Mo_{18}^{6-} , W_{18}^{6-} , or TPSHFA to MB of 5:1; or at a molar ratio of $\text{H}_3\text{PW}_{12}\text{O}_{40}$ to MB ranging from 1:2.5 to 5:1) was added.

UV–vis absorption spectra were obtained on quartz slides using a Perkin-Elmer UV–vis Lambda 40 spectrophotometer. FTIR transmittance spectra (at 4 cm^{-1} resolution and 128 scans) were recorded on silicon wafers using a Bruker, Tensor 27 spectrometer. NMR 1D and 2D spectra were run on a Bruker Avance 500 MHz instrument using standard pulse sequences, in $\text{DMSO}-d_6$ at 25 °C. The samples analyzed with NMR spectroscopy were either solutions of powders of compounds (PHEMA and POMs) or solutions of flakes obtained from scrubbing of POM-containing PHEMA films. The thicknesses of the polymeric films were measured using an Ambios technology XP-2 profilometer.

In a typical film preparation process, the POM-containing PHEMA films were spin coated (at 3000 rpm) onto silicon wafers or quartz slides. In a subsequent curing step, the films formed (60–280 nm thick) were thermally treated (at a temperature range of 50–200 °C, for 1–5 min). Next, the thermally cross-linked films were incubated in a variety of solvents/solutions (water, ethanol and 0.26 M aqueous solution of TMAH) and times (1–30 min) for the POM removal. In the case where a PAG (TPSHFA) was added within PHEMA films (for the study of the MB protonation presented in Supporting Information) the films were exposed through a 248 nm narrow band filter (7 nm bandwidth at half-maximum) using a deep UV Orial Hg–Xe, 500W exposure tool.

Results and Discussion

1. Thermal Reduction of POMs within PHEMA Films.

a. UV Monitoring of Mo_{18}^{6-} Thermal Reduction. For the investigation of the thermally induced acid generation by both Dawson-type POMs (Mo_{18}^{6-} and W_{18}^{6-}) through their thermal reduction within PHEMA films, the monitoring of their thermal reduction was inevitably the first step of the study. Thus, the thermal reduction of POMs within PHEMA films was followed with UV–vis and FTIR spectroscopy, since these methods are the most

suitable for the monitoring of chemical reactions inside polymeric films. The thermal reduction of the Mo_{18}^{6-} ions was initially studied, as the reduced ions obtained are not reoxidized by oxygen and characteristic absorption bands indicative of their reduction are formed.^{7,27} On the other hand, the reduction of the W_{18}^{6-} ions could not be followed spectrophotometrically under ambient conditions because of their rapid reoxidation by oxygen.^{7,27,28} In the case of the Mo_{18}^{6-} ions, it was found that they are gradually reduced upon increase of temperature from 70 to 150 °C, within PHEMA films, as shown from the progressive increase in the intensity of the intervalence charge transfer (IVCT: $\text{Mo}^{\text{V}} \rightarrow \text{Mo}^{\text{VI}}$) band of the ions and the shift of that band to lower wavelengths (782 \rightarrow 746 nm; Figure 1a). It is believed, on the basis of the absorbance peak position, that at 140 °C almost all of the Mo_{18}^{6-} ions have been converted to the two-electron heteropoly blues (Mo_{18}^{8-} species). The position of the IVCT band of the ions reaches 759 nm under these conditions (the assignment of the IVCT band is based on previous results in solution).²⁹ At 150 °C, the thermal reduction of the two-electron reduced Mo_{18}^{8-} ions proceeds further, that is, it seems that a small percentage of those ions have been converted to the four-electron reduced Mo_{18}^{10-} species (which is known as the next stable reduced species). The above thermal reduction of the Mo_{18}^{6-} ions within PHEMA films is in agreement with previous experimental findings reporting that the Mo_{18}^{6-} ions are thermally reduced by an organic compound (such as α -tocopherol³⁰ and ascorbic acid³¹) with about $4e^-$ (through $2e^-$ -addition steps), in both micelles and alcoholic solutions. Furthermore, the change of the IVCT band during the thermal reduction of the Mo_{18}^{6-} ions within PHEMA

(27) Hiskia, A.; Papaconstantinou, E. *Inorg. Chem.* **1992**, *31*, 163.

(28) Argitis, P.; Papaconstantinou, E. *J. Photochem.* **1985**, *30*, 445.

(29) Papaconstantinou, E.; Pope, M. T. *Inorg. Chem.* **1970**, *9*, 667.

(30) Papaconstantinou, E.; Paleos, C. M. *Inorg. Chim. Acta* **1986**, *125*, L5.

(31) Paleos, C. M.; Papaconstantinou, E. *J. Colloid Interface Sci.* **1986**, *113*, 297.

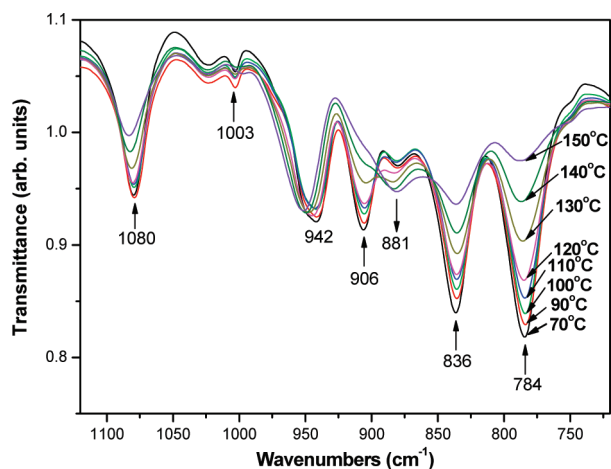


Figure 2. FTIR monitoring of the thermal reduction of the Mo_{18}^{6-} ions within PHEMA films, in the temperature range of 70 to 150 °C. The thermal treatment temperatures (°C) and the positions (cm^{-1}) of the FTIR peaks of the Mo_{18}^{6-} ions are indicated on spectra. (Solution Mo_{18}^{6-} -PHEMA, 53.4–6.28% (w/w EL). Thermal treatment time, 5 min. Initial film thickness, 279 nm.).

films is very similar to the change of that band during the photoreduction of the ions within PHEMA films,¹⁸ as well as throughout the photoreduction of the ions in aqueous solutions of alcohols.³²

The reduction of the Mo_{18}^{6-} ions upon increase of temperature in the range of 70 to 150 °C, within PHEMA films, is also evidenced by the decrease in the intensity of the oxygen-to-metal charge transfer (OMCT: $\text{O} \rightarrow \text{Mo}$) band of the ions and the shift of that band to higher wavelengths (215 \rightarrow 220 nm; Figure 1b). Similar change of the OMCT band was also reported in the literature during the electrochemical reduction of the Mo_{18}^{6-} ions in solution.²⁹ On the other hand, it was found that at elevated temperatures ($T > 150$ °C) the thermal reduction of the Mo_{18}^{6-} ions does not proceed further.

b. FTIR Monitoring of Mo_{18}^{6-} Thermal Reduction. The reduction of the Mo_{18}^{6-} ions with the increase of temperature in the range of 70 to 150 °C, within PHEMA films, was also studied with FTIR spectroscopy (Figure 2). Upon increase of temperature in the above range, the following changes in the FTIR peaks of the Mo_{18}^{6-} ions (assigned according to literature)³³ were observed: (a) decrease in the intensity of the asymmetric stretching of the $\text{P}-\text{O}_a$ bonds (1080 and 1003 cm^{-1}); (b) decrease in the intensity of the asymmetric stretching of the $\text{Mo}-\text{O}_b-\text{Mo}$ bridges (906 cm^{-1}); (c) decrease in the intensity of the asymmetric stretching of the $\text{Mo}-\text{O}_c-\text{Mo}$ bridges (836 and 784 cm^{-1}).³⁴ The decrease in the intensity of the aforementioned bonds upon increase of temperature indicates that those bonds are possibly

dissociated, as expected when the Mo_{18}^{6-} ions are reduced. Indeed, previous experimental findings have shown dissociation of both $\text{P}-\text{O}_a$ bonds and $\text{Mo}-\text{O}_{b,c}-\text{Mo}$ bridges during the photoreduction of the Mo_{18}^{6-} ions within PHEMA films.¹⁸ Similar results have been reported for the reduction of the Keggin-type 12-molybdophosphate ions, $[\text{PMo}_{12}\text{O}_{40}]^{3-}$, in solution.^{35,36} In addition, it is interesting that upon increase of temperature in the same range the asymmetric stretching of the $\text{Mo}=\text{O}_d$ bonds (942 cm^{-1}) remains almost constant in intensity indicating that those bonds are practically unaffected. This result is also in agreement with a previous finding in literature reporting that the $\text{Mo}=\text{O}_d$ bonds are not reactive until the $4e^-$ reduction of the similar $[\text{PMo}_{12}\text{O}_{40}]^{3-}$ ions.³⁵

On the other hand, the small, non-systematic shift of the $\text{Mo}=\text{O}_d$ bonds observed probably originates from changes in the intermolecular interactions with the polymer (see also Figure 5a and discussion in section 3a on PHEMA cross-linking). Also, another significant point is that a new band (at ~ 881 cm^{-1}) appears during the thermal reduction of the Mo_{18}^{6-} ions within PHEMA films. That band could be possibly attributed to the formation of a new kind of $\text{Mo}-\text{O}-\text{Mo}$ bridges, presumably stemming from the aforementioned dissociation of the $\text{Mo}-\text{O}_{b,c}-\text{Mo}$ bridges. The whole issue needs further investigation (with the use of additional techniques, such as XPS, ESR, and electrochemical methods).

c. Kinetic Study of the Thermally-Induced, $2e^-$ -Reduction of Mo_{18}^{6-} . To have a clear view of the thermally induced, $2e^-$ -reduction of the Mo_{18}^{6-} ions within PHEMA films, the kinetics of the reaction in the temperature range of 110 to 130 °C was investigated. At a temperature lower than 110 °C the reaction proceeds very slowly because of the relatively high glass transition temperature ($T_g \sim 90$ °C) of PHEMA,³⁷ whereas at a temperature higher than 130 °C (up to 150 °C) the reaction proceeds very quickly. Thus, the change in the absorption intensity of the IVCT band of the Mo_{18}^{6-} ions at 758 nm (i.e., the change in the concentration of the $2e^-$ -reduced Mo_{18}^{8-} ions) in the above temperature range, versus the thermal treatment time, was studied (Figure 3). As shown in this Figure, at a constant temperature, upon increase of thermal treatment time the concentration of the $2e^-$ -reduced Mo_{18}^{8-} ions increases initially linearly (pseudo-first-order reaction with respect to the Mo_{18}^{6-} ions) moving progressively to saturation. By assuming that the studied reaction follows pseudo-first-order kinetics (i.e., the reaction rate depends exclusively on the concentration of the Mo_{18}^{6-} ions, and not on the concentration of PHEMA hydroxyls, which is in excess of the concentration of the Mo_{18}^{6-} ions; initial molar ratio of Mo_{18}^{6-} /PHEMA hydroxyls, 1:19), the reaction rate constant (k) at each temperature can be derived from the initial reaction rate.

(32) Papaconstantinou, E.; Dimotikali, D.; Politou, A. *Inorg. Chim. Acta* **1980**, *46*, 155.

(33) Yang, G.; Gong, J.; Yang, R.; Guo, H.; Wang, Y.; Liu, B.; Dong, S. *Electrochem. Commun.* **2006**, *8*, 790.

(34) O_a represents the central oxygens of the Dawson structure of the Mo_{18}^{6-} ions; O_b represents the oxygens that belong to different Mo_3O_{13} triads and bridge the corner-sharing MoO_6 octahedra; O_c represents the oxygens that belong to the same Mo_3O_{13} triad and bridge the edge-sharing MoO_6 octahedra; O_d represents the terminal oxygens of the Dawson structure.

(35) Eguchi, K.; Toyozawa, Y.; Yamazoe, N.; Seiyama, T. *J. Catal.* **1983**, *83*, 32.

(36) Taketa, H.; Katsuki, S.; Eguchi, K.; Seiyama, T.; Yamazoe, N. *J. Phys. Chem.* **1986**, *90*, 2959.

(37) Çayakara, T.; Özyürek, C.; Kantoğlu, Ö. *J. Appl. Polym. Sci.* **2007**, *103*, 1602.

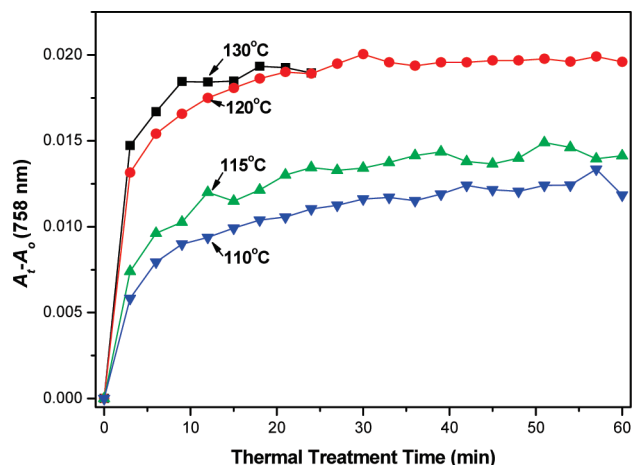


Figure 3. Change in the absorption intensity of the IVCT band (at 758 nm) of the $2e^-$ -reduced Mo_{18}^{8-} ions during the thermal treatment of the Mo_{18}^{6-} -PHEMA films, upon thermal treatment time. The thermal treatment of the films was performed in the temperature range of 110 to 130 °C, through steps of 3 min time. (Solution Mo_{18}^{6-} -PHEMA, 53.9–3.11% (w/w EL). Initial film thickness range, 79–107 nm.).

Subsequently, the activation energy (E_a) of the studied reaction (in the temperature range of 110 to 130 °C) was estimated from the slope of the line of the plot of $\log k$ versus $1/T$, according to the empirical Arrhenius equation:

$$k = Ae^{-E_a/RT} \quad (1)$$

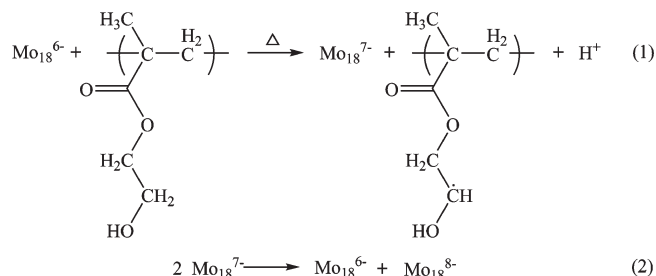
or

$$\log k = \log A - E_a/(2.3RT) \quad (2)$$

The E_a was found to be equal to 62 kJ mol $^{-1}$ (frequency factor, $A \sim 6.4 \times 10^5 \text{ min}^{-1}$). That E_a value is comparable with the E_a values reported in literature for the oxidation (by POMs) of other organic compounds containing hydroxyl groups.³⁸

d. Discussion on the Thermal Reduction Mechanism of Mo_{18}^{6-} within PHEMA films. From the spectrophotometric data previously shown, the two-electron reduced Mo_{18}^{8-} ions were detected within PHEMA films at 140 °C in the time domain of our investigation. It is believed that the $2e^-$ -reduced Mo_{18}^{8-} ions are formed by the reduction of the initial Mo_{18}^{6-} ions to the $1e^-$ -reduced Mo_{18}^{7-} ions, which are rapidly disproportionated to the initial Mo_{18}^{6-} ions and the $2e^-$ -reduced Mo_{18}^{8-} ions (Scheme 1). Although the disproportionation of the Mo_{18}^{7-} ions (reaction 2) is more limited in polymer films than in solution, it is expected to be very effective in films at the elevated temperatures of this study. At a higher temperature (i.e., at 150 °C) the reduction of the $2e^-$ -reduced Mo_{18}^{8-} ions proceeds further, (i.e., a small percentage of those ions are converted to the $4e^-$ -reduced Mo_{18}^{10-} ions). Also, from experimental data subsequently presented (see Figure 5a and discussion in section 3a on PHEMA cross-linking) it was

Scheme 1. Mechanism of Thermally-Induced Acid Generation by the Mo_{18}^{6-} Ions within PHEMA Films, at $T \leq 150$ °C



found that initially the Mo_{18}^{6-} ions are preassociated with PHEMA molecules through intermolecular hydrogen bonding interactions. This observation has been repeatedly reported in solution studies in the literature,^{7,8,25,30} but in the present work a clear experimental evidence of this fact in films is provided. The proposed mechanism is generally similar to the mechanism reported in the literature for the thermal^{30,31} and photochemical^{7,25} reduction of POMs by organic compounds in solution. An analogous reaction mechanism can be written for the thermal reduction of the W_{18}^{6-} ions within PHEMA films, but in that case, the thermal reduction is expected to proceed through $1e^-$ addition steps.^{28,29} Finally, from the proposed mechanism, it is evident that protons are produced by the thermal reduction of the Mo_{18}^{6-} ions (and the W_{18}^{6-} ions as well) within PHEMA films. The capture of the produced protons by the $2e^-$ -reduced Mo_{18}^{8-} ions depends on the basicity of the medium. In the next sections, it will be examined, if the produced protons are available (under the conditions of our investigation) for the protonation of a suitable acid indicator and for the catalysis of PHEMA cross-linking.

2. Acid Generation Monitoring. The acid generated by the thermal reduction of both POMs investigated within PHEMA films, was detected with the addition of a known acid indicator (methylene blue, MB) and monitoring the indicator's protonation with UV spectroscopy. The protonation of MB follows the reaction sequence:



according to the literature.³⁹ Initially, the MB is in its unprotonated form, MB^+ , in equilibrium with its dimer, $[\text{MB}^+ \cdots \text{MB}^+]$ (reaction eq 3). The generation of acid in the system shifts the two equilibrium reactions to the right, forming the protonated form of MB, MBH^{2+} (reaction eq 4). The protonation of MB is easily monitored with UV spectroscopy, where gradual disappearance of the MB^+ peak (665 nm) and its dimer's peak (611 nm) and appearance of a new peak ascribed to the protonated form MBH^{2+} (762 nm) can be observed. Indeed, those spectral changes of MB protonation were first detected

(38) (a) Gaspar, A.; Evtuguin, D. V.; Neto, C. P. *Appl. Catal.*, **A** **2003**, 239, 157. (b) Arslan-Alaton, I.; Ferry, J. L. *Dyes Pigm.* **2002**, 54, 25.

(39) (a) Kiwi, J.; Denisov, N.; Nadtochenko, V. *J. Phys. Chem. B* **1999**, 103, 9141. (b) Bergmann, K.; O'Konski, C. T. *J. Phys. Chem.* **1963**, 67, 2169.

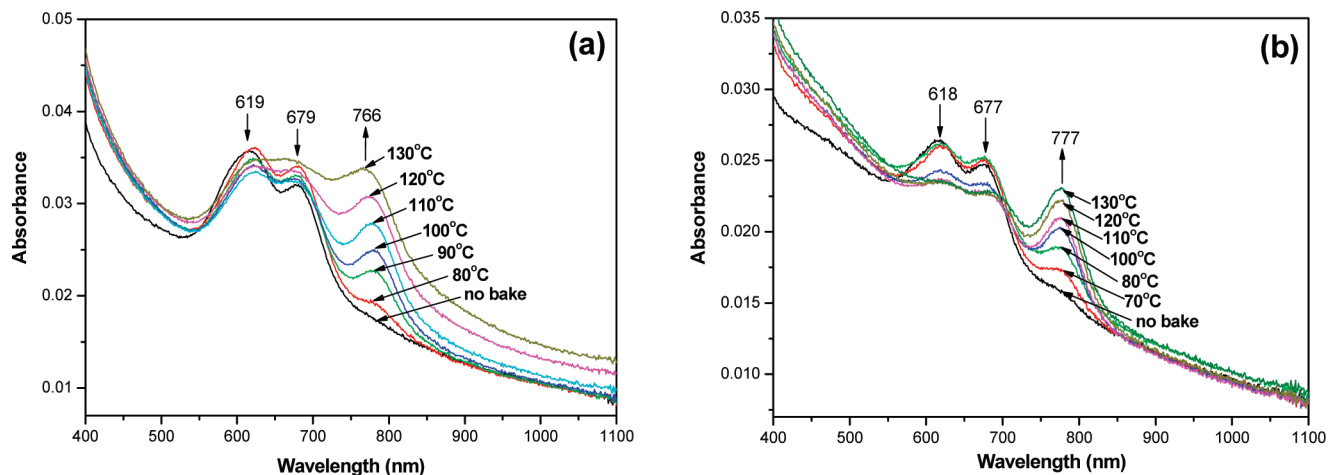


Figure 4. UV monitoring of MB protonation caused by the thermal acid generation of (a) the Mo_{18}^{6-} ions and (b) the W_{18}^{6-} ions, within PHEMA films. Thermal treatment temperature: (a) 80–130 °C, (b) 70–130 °C. ((a) Solution Mo_{18}^{6-} -MB-PHEMA, 0.11–1.41–2.5% (w/w DMSO); molar ratio Mo_{18}^{6-} /MB, 5:1. (b) Solution W_{18}^{6-} -MB-PHEMA, 0.29–1.04–2.5% (w/w DMSO); molar ratio W_{18}^{6-} /MB, 5:1. Thermal treatment time, 1 min.).

within PHEMA films, in two cases used for the control of our methodology: (a) with the addition of a known PAG (triphenylsulfonium hexafluoroantimonate, TSPHFA)^{19c,d} and the subsequent 248 nm irradiation of the films, and (b) with the gradual addition of a solid acid (12-tungstophosphoric acid, $\text{H}_3\text{PW}_{12}\text{O}_{40}$) within the films (both results are presented in the Supporting Information).

Similar spectral changes of MB were observed during the monitoring of the thermally induced acid generation by both Dawson-type POMs within PHEMA films (Figure 4). The only difference was the small shift in the peaks of the involved species (MB^+ , dimer and protonated form). Indeed, in the case of the Mo_{18}^{6-} ions, upon increase of temperature up to 130 °C (i.e., approximately until the $2e^-$ reduction of the ions according to Figure 1a) both peaks of MB^+ and its dimer (679 and 619 nm, respectively) decrease, whereas a broadened peak (766 nm) attributed to the protonated form MBH^{2+} gradually appears (Figure 4a). In this case, the appearance of the MBH^{2+} peak (and the rest spectral changes of MB as well) is not as evident as the one observed in the case of TSPHFA and $\text{H}_3\text{PW}_{12}\text{O}_{40}$ because of the considerable overlap of the protonated MBH^{2+} peak with the broad IVCT band of the reduced Mo_{18}^{6-} ions.

Similar, but more evident, spectral changes of MB were observed in the case of the W_{18}^{6-} ions (Figure 4b). In particular, upon increase of temperature up to 130 °C, both peaks of MB^+ and its dimer (677 and 618 nm respectively) decrease more distinguishably, whereas a clear, sharp peak (777 nm) ascribed to the protonated MBH^{2+} progressively emerges. The clear distinction of the MBH^{2+} peak in the case of the W_{18}^{6-} ions stems from the rapid and complete reoxidation of the POM ions by oxygen.^{7,27,28} Thus, although the thermal reduction of the W_{18}^{6-} ions within PHEMA films could not be spectrophotometrically followed under ambient conditions, the thermally induced acid generation by those ions is clearly evidenced with the use of the acid indicator.

3. Thermal Curing of PHEMA Films. *a. FTIR Study of PHEMA Cross-Linking.* Having proved the thermally

induced acid generation by both POMs within PHEMA films, the cross-linking of PHEMA was subsequently investigated. As it has been reported in the literature, PHEMA is catalytically cross-linked in the presence of acid, mainly through a transesterification mechanism.⁴⁰ In the current study, the PHEMA cross-linking was first evidenced by the solubility change of the POM-PHEMA films upon thermal treatment. Indeed, thermal treatment of the Mo_{18}^{6-} -PHEMA films at 110 °C for 2 min resulted in insolubilization of the films in water. In a similar way, the W_{18}^{6-} -PHEMA films turned insoluble in water upon thermal treatment at 120 °C for 2 min.

The results of the dissolution studies were subsequently supported with FTIR spectroscopy. From the FTIR study of the thermally treated Mo_{18}^{6-} -PHEMA films, the following changes in the PHEMA peaks were observed (Figure 5a; the FTIR peaks of PHEMA are assigned according to literature).⁴¹ (a) Initially, prior to the thermal treatment and because of the presence of the Mo_{18}^{6-} ions within the PHEMA films, the O–H stretching peak of PHEMA clearly splits into two peaks ($3435 \rightarrow 3502, 3272 \text{ cm}^{-1}$; curves A, B) and the C=O stretching peak shifts to lower wavenumbers ($1728 \rightarrow 1725 \text{ cm}^{-1}$). This is clear evidence that the Mo_{18}^{6-} ions are preassociated with PHEMA molecules through intermolecular hydrogen bonding interactions. Specifically, the two O–H peaks at 3502 and 3272 cm^{-1} are assigned to the non-hydrogen bonded and hydrogen bonded OH stretching vibrations, respectively.⁴¹ That finding is in agreement with previous literature reports that both the thermal³⁰ and the photochemical^{7,8,25} oxidation of organic compounds by POMs in solution (and within PHEMA films

(40) (a) Vasilopoulou, M.; Boyatzis, S.; Raptis, I.; Dimotikalli, D.; Argitis, P. *J. Mater. Chem.* **2004**, *14*, 3312. (b) Lee, J.; Aoi, T.; Kondo, S.; Miyagawa, N.; Takahara, S.; Yamaoka, T. *J. Polym. Sci., Part A: Polym. Chem.* **2002**, *40*, 1858.

(41) (a) Perova, T. S.; Vij, J. K.; Xu, H. *Colloid Polym. Sci.* **1997**, *275*, 323. (b) Ji, X.-L.; Jiang, S.-C.; Qiu, X.-P.; Dong, D.-W.; Yu, D.-H.; Jiang, B.-Z. *J. Appl. Polym. Sci.* **2003**, *88*, 3168. (c) Luciani, G.; Constantini, A.; Silvestri, B.; Tescione, F.; Branda, F.; Pezzella, A. *J. Sol-Gel Sci. Technol.* **2008**, *46*, 166.

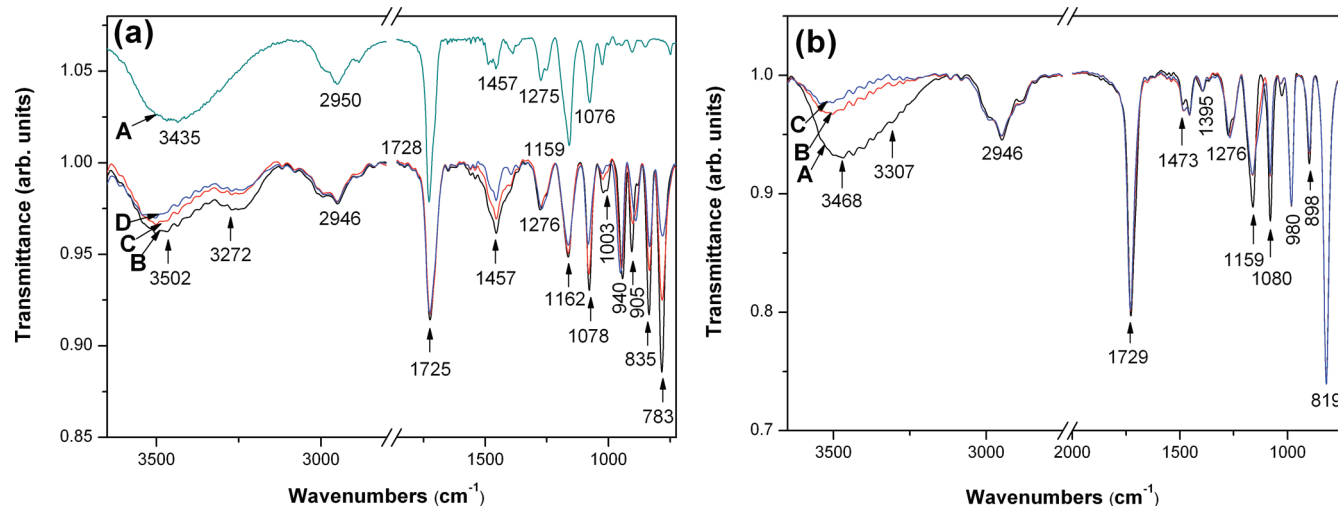


Figure 5. FTIR study of PHEMA cross-linking in the following: (a) a Mo_{18}^{6-} -PHEMA film, (b) a PHEMA film containing the heteropoly acid, $\text{H}_3\text{PW}_{12}\text{O}_{40}$. In (a): curve A, a PHEMA film (not thermally treated); curve B, the initial Mo_{18}^{6-} -PHEMA film (not thermally treated); curve C, thermal treatment of the latter film at 140 °C, for 5 min; curve D, thermal treatment of the latter film at 140 °C, for 60 min. In (b), curve A, the initial $\text{H}_3\text{PW}_{12}\text{O}_{40}$ -PHEMA film (not thermally treated); curve B, thermal treatment at 140 °C, for 5 min; curve C, thermal treatment at 140 °C, for 60 min. ((a) Solution Mo_{18}^{6-} -PHEMA, 50–5% (w/w MeOH); initial film thickness, 204 nm. (b) Solution $\text{H}_3\text{PW}_{12}\text{O}_{40}$ -PHEMA, 50–5% (w/w MeOH); initial film thickness, 294 nm).

as well)¹⁸ proceeds through preassociation of POM with the organic compound. (b) Upon thermal treatment of the films at 140 °C for 5 min (i.e., until the $2e^-$ reduction of the Mo_{18}^{6-} ions according to Figure 1a) the following changes in the PHEMA peaks were observed (curve C): considerable decrease in the intensity of both O–H stretching peaks (3502, 3272 cm^{-1}), and in particular, the decrease of the hydrogen bonded OH band (3272 cm^{-1}) is greater than the decrease of the non-hydrogen bonded OH peak (3502 cm^{-1}); decrease in the intensity of the C=O stretching peak (1725 cm^{-1}); decrease in the intensity of the CH_2 in-plane bending peak (1457–1496 cm^{-1}); decrease in the intensity of the C–O stretching peak (1162 cm^{-1}); significant decrease in the peak (1078 cm^{-1}) attributed to both C–O–C stretching and P–O_a asymmetric stretching of POM. The above FTIR changes indicate that acid-catalyzed cross-linking of PHEMA takes place at that temperature, as it will be discussed in the next paragraph. (c) Upon longer thermal treatment at 140 °C (i.e., for 60 min), similar FTIR changes were also observed (curve D).

Analogous, but more intense, FTIR changes were also observed during the thermal treatment of PHEMA films containing the heteropoly acid, $\text{H}_3\text{PW}_{12}\text{O}_{40}$ (Figure 5b). That result is an additional proof that PHEMA cross-linking proceeds through an acid catalyzed, ester thermolysis mechanism. Among the two most common acid-catalyzed cross-linking mechanisms of PHEMA reported in the literature (i.e., transesterification and etherification), the aforementioned FTIR changes of PHEMA support the transesterification mechanism.⁴⁰ Similar FTIR changes were also detected in the W_{18}^{6-} -PHEMA films (Supporting Information). The only difference in that case is that the split of the OH stretching band into two peaks as a result of the presence of the W_{18}^{6-} ions is apparently less intense than the split of the OH band previously found in the Mo_{18}^{6-} -PHEMA films. That

finding indicates that the hydrogen bonding interactions between W_{18}^{6-} and PHEMA are less strong than the corresponding interactions between Mo_{18}^{6-} and PHEMA, possibly because the Mo–O bonds are more polarized than the W–O bonds.⁵ A further evidence that PHEMA cross-linking results from the thermally induced acid generation by both Mo_{18}^{6-} and W_{18}^{6-} ions, and not, for instance, from a thermal intramolecular reaction of the polymer, is provided with an FTIR study of POM-free PHEMA films. That study showed lack of PHEMA cross-linking reactions for thermal treatment up to 197 °C (Supporting Information).

b. NMR Study of PHEMA Cross-Linking. The thermal curing of POM-containing PHEMA films was also studied with ^1H NMR spectroscopy. Initially, the ^1H NMR peaks of PHEMA (CH_3 : δ = 0.77, 0.94 ppm; CH_2 (main chain): 1.15, 1.23, 1.78 ppm; $-\text{CH}_2\text{OH}$: 3.58 ppm; $-\text{O}-\text{CH}_2$: 3.89 ppm; OH: 4.80 ppm; in $\text{DMSO}-d_6$; curve A, Figure 6a) were assigned after obtaining the 2D ^1H – ^{13}C multiplicity-edited HSQC NMR spectrum of PHEMA (Supporting Information). The ^1H NMR peaks of PHEMA are in accordance with those reported in literature.⁴² Upon mixing Mo_{18}^{6-} ions and PHEMA (separately, not within films) in $\text{DMSO}-d_6$ solution, small changes were observed in the ^1H NMR spectrum (curve B, Figure 6a): small increase of CH_2 peak (1.23 ppm); appearance of a small, broad peak (6.69 ppm) attributed to NH_4^+ ions; emergence of remote OH peaks (6.65, 7.19 ppm). Those changes evidence the presence of NH_4^+ counterions and hydrogen bonding interactions between Mo_{18}^{6-} and OH groups, but they do not support a possible reaction between Mo_{18}^{6-} and PHEMA in solution.

The picture was completely different when the Mo_{18}^{6-} ions were introduced into PHEMA films and the films

(42) (a) Reining, B.; Keul, H.; Höcker, H. *Polymer* **2002**, *43*, 3139. (b) Cao, Z.; Liu, W.; Ye, G.; Zhao, X.; Lin, X.; Gao, P.; Yao, K. *Macromol. Chem. Phys.* **2006**, *207*, 2329.

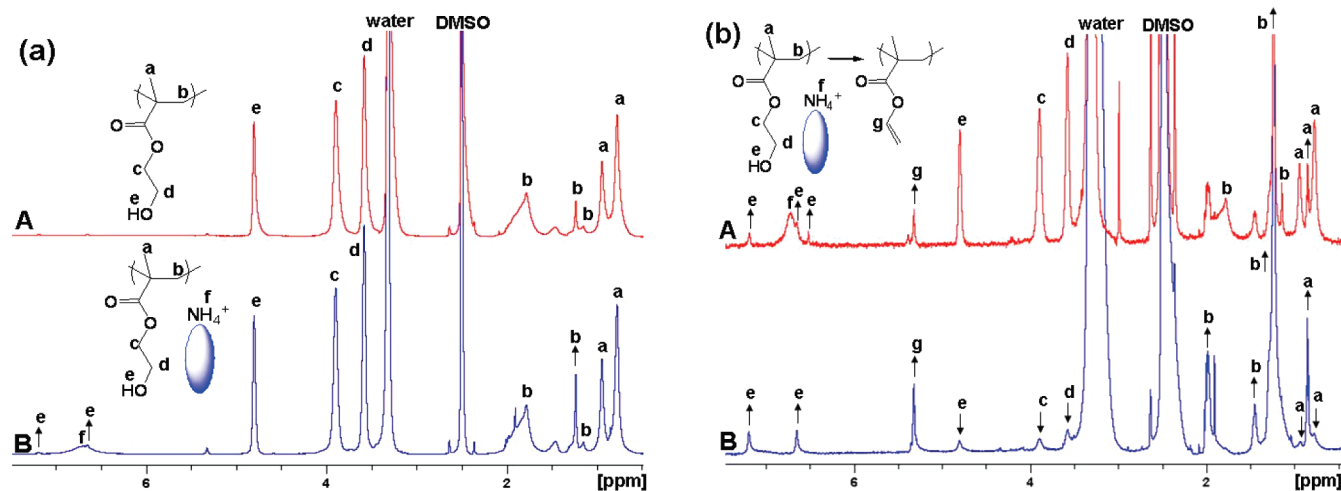


Figure 6. ^1H NMR study of PHEMA cross-linking by the Mo_{18}^{6-} ions: (a) in solution, (b) in films (both dissolved in $\text{DMSO}-d_6$). In (a): curve A, a PHEMA solution; curve B, a Mo_{18}^{6-} -PHEMA solution. In (b): curve A, the initial Mo_{18}^{6-} -PHEMA film (not thermally treated); curve B, thermal treatment of the film at 140°C , for 5 min. ((b) Solution for the preparation of Mo_{18}^{6-} -PHEMA films: curve A, 52.5–3.11% (w/w EL); curve B, 50–5% (w/w EL).).

were subsequently dissolved in $\text{DMSO}-d_6$, where the following changes were detected (curve A, Figure 6b): emergence of a new peak (0.85 ppm) assigned to CH_3 ; major increase of the CH_2 peak (1.23 ppm); appearance of a new peak (5.32 ppm) assigned to $\text{CH}=\text{C}$ peak as evidenced in the next paragraph; considerable increase of the remote OH peaks (6.52, 6.65, 7.19 ppm). The latter changes indicate that dehydration of PHEMA along with extended hydrogen bonding interactions between Mo_{18}^{6-} and PHEMA take place inside the Mo_{18}^{6-} -PHEMA films at ambient temperature. In addition, an important finding obtained with UV spectroscopy (data not shown) was that the Mo_{18}^{6-} ions are capable to oxidize a small percentage of OH groups within PHEMA films at ambient temperature generating therefore, a low concentration of acid according to Scheme 1. It is highly possible that the generated acid initiates the aforementioned PHEMA dehydration, whereas it can not initiate PHEMA cross-linking reactions at this temperature, since the films are completely soluble in $\text{DMSO}-d_6$.

Upon thermal treatment of the Mo_{18}^{6-} -PHEMA films at 140°C , PHEMA is cross-linked to such a degree that the films turned almost insoluble in $\text{DMSO}-d_6$ (less than 10% of the films were dissolved in that solvent). Thus, the NMR spectra obtained subsequently to the thermal treatment of the films provide evidence only for side reactions that lead to the formation of soluble products, and not for the main PHEMA cross-linking reaction. In particular, the following ^1H NMR changes were observed (curve B, Figure 6b): approximately the disappearance of the initial CH_3 peaks (0.77, 0.93 ppm) and significant increase of a new CH_3 peak (0.85 ppm); huge increase of one CH_2 peak (1.23 ppm) and significant increase of two new CH_2 peaks (1.45, 1.98 ppm); almost entire decrease of the $-\text{CH}_2\text{OH}$, $-\text{O}-\text{CH}_2$ and OH peaks (3.57, 3.89, and 4.80 ppm, respectively); major increase of a peak (5.32 ppm) assigned to $\text{CH}=\text{C}$ peak, since this proton corresponds to a methine and associates with a carbon at 129 ppm (see the 2D $^1\text{H}-^{13}\text{C}$ multiplicity-edited HSQC NMR spec-

trum of this film in Supporting Information); increase of the remote OH peaks (6.65, 7.19 ppm). From the latter ^1H NMR changes, it is apparent that the side reaction (in relation to the main acid-catalyzed cross-linking reaction of PHEMA) is PHEMA dehydration, which takes place to a high degree at 140°C . The vinyl end groups formed after PHEMA dehydration possibly give soluble (in $\text{DMSO}-d_6$) cyclization products, which could be responsible for the major increase of the CH_2 peak (1.23 ppm).

To confirm that the aforementioned changes of the Mo_{18}^{6-} -PHEMA films are acid-catalyzed, PHEMA films with embedded molecules of the heteropoly acid $\text{H}_3\text{PW}_{12}\text{O}_{40}$ were also studied with ^1H NMR spectroscopy. Initially, when the heteropoly acid and PHEMA were dissolved separately (not within films) in $\text{DMSO}-d_6$, the complete disappearance of the OH peak (4.80 ppm; Figure 7a) along with a relatively small increase of the CH_2 peak (1.23 ppm) were detected. Those changes clearly indicate that an acid-catalyzed, hydroxyl group eliminating reaction (e.g., transesterification) of PHEMA occurs in solution at ambient temperature, a reaction that must be intramolecular, since it does not result in PHEMA cross-linking. On the other hand, when the heteropoly acid was introduced into PHEMA films, similar results to those previously described in the case of the Mo_{18}^{6-} ions (at ambient temperature and upon thermal treatment at 140°C ; curves A,B, Figure 7b) were found. Also, all the findings obtained from the NMR study of the W_{18}^{6-} ions in both solution and PHEMA films (Supporting Information) were completely analogous to those formerly encountered with the Mo_{18}^{6-} ions.

c. Discussion on PHEMA Cross-Linking Mechanism. In brief, from the combination of the previous FTIR and NMR results the following findings regarding the PHEMA cross-linking were obtained. (a) In solution (at ambient temperature), both Mo_{18}^{6-} and W_{18}^{6-} ions do not give a reaction with PHEMA to a significant degree. In contrast, the heteropoly acid ($\text{H}_3\text{PW}_{12}\text{O}_{40}$) gives an acid-catalyzed reaction that eliminates the hydroxyl group of

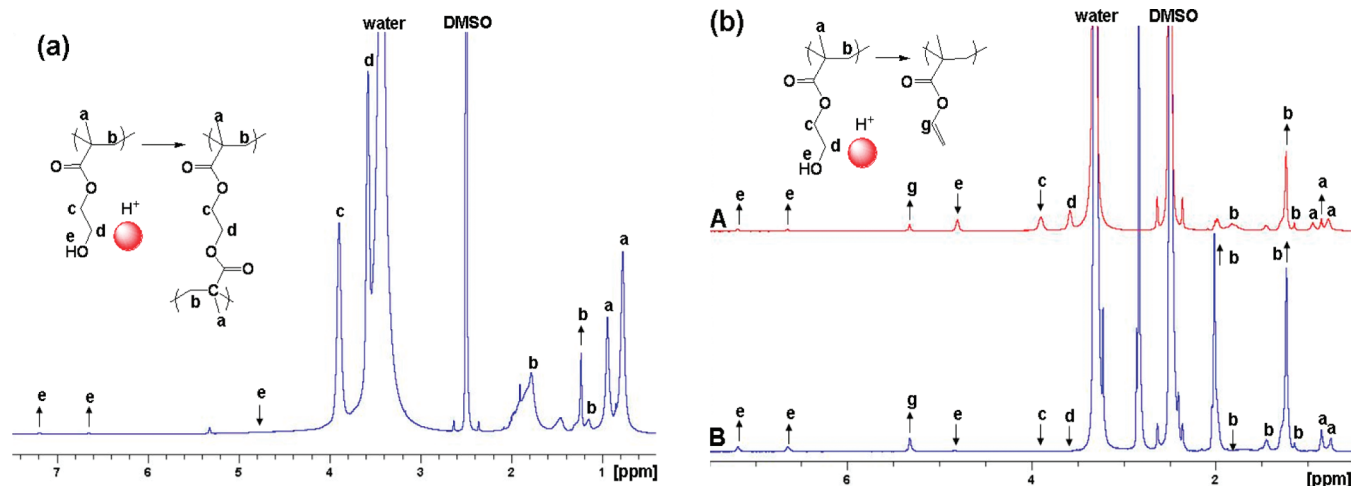
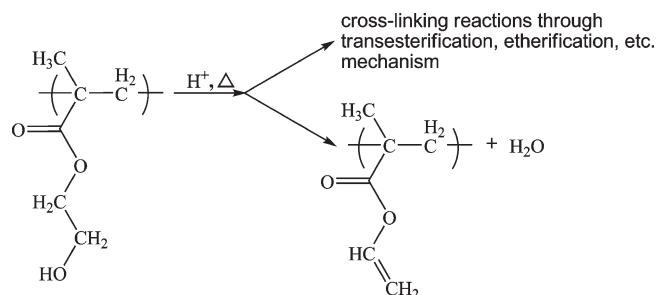


Figure 7. ^1H NMR study of PHEMA cross-linking by the heteropoly acid $\text{H}_3\text{PW}_{12}\text{O}_{40}$: (a) in solution, (b) in films (both dissolved in $\text{DMSO}-d_6$). In (a): an $\text{H}_3\text{PW}_{12}\text{O}_{40}$ -PHEMA solution. In (b): curve A, the initial $\text{H}_3\text{PW}_{12}\text{O}_{40}$ -PHEMA film (not thermally treated); curve B, thermal treatment of the film at $140\text{ }^\circ\text{C}$, for 5 min. ((b) Solution for the preparation of $\text{H}_3\text{PW}_{12}\text{O}_{40}$ -PHEMA films, 50–4% (w/w MeOH)).

Scheme 2. Acid-Catalyzed Cross-Linking of PHEMA Followed by the Side Reaction of Acid-Catalyzed Dehydration of PHEMA



PHEMA (e.g., transesterification, etherification, etc.), a reaction that does not result in PHEMA cross-linking in solution. (b) In films, at ambient temperature, both Mo_{18}^{6-} and W_{18}^{6-} ions give acid-catalyzed dehydration of PHEMA (Scheme 2) that leads to the formation of soluble (in $\text{DMSO}-d_6$) possibly cyclization products. In this reaction, the acid is generated by the oxidation of a small percentage of PHEMA hydroxyl groups by the Dawson ions at ambient temperature. The same holds with the heteropoly acid, but in that case a high concentration of acid is initially present inside the films. (c) Upon thermal treatment of POM-PHEMA films at $140\text{ }^\circ\text{C}$, both Mo_{18}^{6-} and W_{18}^{6-} ions give as side reaction (in relation to the main acid-catalyzed cross-linking reaction of PHEMA) the acid-catalyzed dehydration of PHEMA, a reaction that leads to the formation of soluble (in $\text{DMSO}-d_6$) products. The same behavior was observed in the case of the heteropoly acid, as well.

d. POM Removal from Thermally Cross-Linked POM-PHEMA Films. The removal of POMs from the thermally cross-linked POM-PHEMA films was investigated by following the OMCT band of POMs after the incubation of the films in various solvents/solutions. In particular, in the case of the Mo_{18}^{6-} -PHEMA film, which was initially thermally treated at $140\text{ }^\circ\text{C}$ (curve A, Figure 8a), the following results were obtained. (a) Upon incubation of the film in water, 53% of the OMCT band of the

Mo_{18}^{6-} ions at 218 nm decreases (curve B, Figure 8a) indicating a similar decrease in the concentration of the ions inside the film. By comparing that result with a previous finding obtained from a photochemically cross-linked Mo_{18}^{6-} -PHEMA film (where the Mo_{18}^{6-} ions were entirely removed from the cross-linked film upon incubation in water),¹⁸ it is obvious that the PHEMA cross-linking reaction proceeds more in the case of the thermally cross-linked film. (b) The incubation in ethanol results in further decrease (61%; curve C, Figure 8a) in the concentration of the Mo_{18}^{6-} ions. (c) Upon incubation in a 0.26 M aqueous solution of TMAH, the Mo_{18}^{6-} ions are completely removed from the film (curve D, Figure 8a) causing also a 54% decrease in the film thickness. The removal of the Mo_{18}^{6-} ions from the thermally cross-linked Mo_{18}^{6-} -PHEMA films upon incubation in a solution of TMAH base (but not upon incubation in water or an organic solvent such as ethanol) probably indicates that the cross-linking of PHEMA is so effective that it does not allow the removal of the Mo_{18}^{6-} ions from the polymer matrix, unless the structure of the ions is destroyed with the use of base.⁴³

Analogous results regarding the effect of the above solutions (water, ethanol, and 0.26 M TMAH aqueous solution) on a thermally cross-linked Mo_{18}^{6-} -PHEMA film were also obtained by following the FTIR peaks of the Mo_{18}^{6-} ions ($1080\text{--}782\text{ cm}^{-1}$; Figure 8b). In addition, a significant observation was made during that study. It was found that after the entire removal of the Mo_{18}^{6-} ions from the thermally cross-linked Mo_{18}^{6-} -PHEMA films (upon incubation of the films in the 0.26 M TMAH solution), the split O–H stretching peak of PHEMA is reestablished at one peak ($3498, 3212 \rightarrow 3428\text{ cm}^{-1}$; curves A,D, Figure 8b). That finding is a further proof of the hydrogen bonding interactions between Mo_{18}^{6-} and PHEMA.¹⁸ Similar results regarding the effect of the aforementioned solutions (water, ethanol, and 0.26 M TMAH

(43) Briand, L. E.; Baronetti, G. T.; Thomas, H. J. *Appl. Catal., A* **2003**, 256, 37.

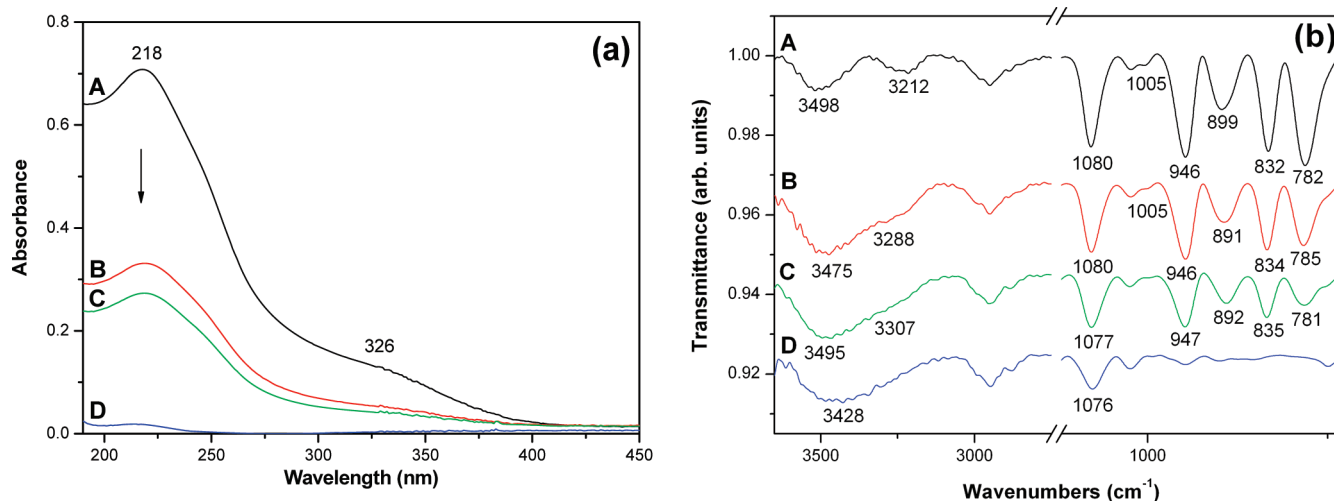


Figure 8. (a) UV and (b) FTIR study showing removal of the Mo_{18}^{6-} ions from thermally cross-linked Mo_{18}^{6-} -PHEMA films, after incubation of the films in various solutions. In (a, b): curve A, the thermally cross-linked Mo_{18}^{6-} -PHEMA film at 140°C ; curve B, incubation in water; curve C, incubation in ethanol; curve D, incubation in a 0.26 M aqueous solution of TMAH. The position of the OMCT bands (218, 326 nm) of the Mo_{18}^{6-} ions within PHEMA films are indicated on the spectra.²⁹ (Solution Mo_{18}^{6-} -PHEMA, 53.9–3.11% (w/w EL). Thermal treatment time, 5 min. Incubation time, 1 min, except for the TMAH solution, in which the time was 30 min. In (a), initial and final film thickness, 72 and 33 nm respectively. In (b), initial and final film thickness, 61 and 46 nm respectively).

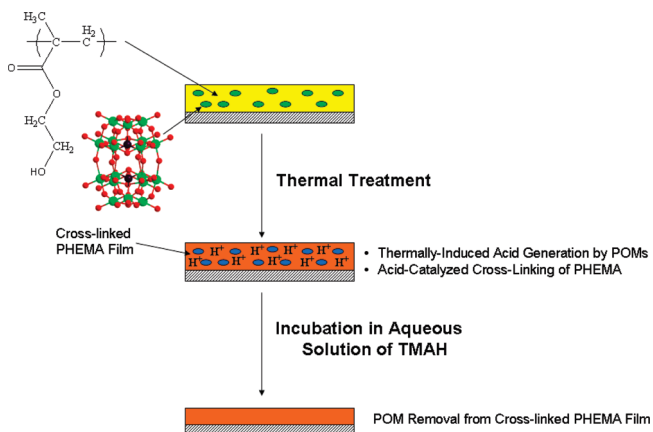


Figure 9. Schematic representation of the two-step thermal curing process of PHEMA films by both POMs investigated.

solution) were also obtained by the UV and FTIR study of the W_{18}^{6-} -PHEMA films (Supporting Information).

From the above study it is apparent that both POMs investigated can be used for the thermal curing of PHEMA films. POMs have a significant advantage in comparison with common thermal curing agents:²¹ they can be completely removed from the thermally (e.g., at 140°C) cross-linked POM-PHEMA films through incubation of the films in an aqueous solution of TMAH (0.26 M), as depicted in the schematic representation of Figure 9. That behavior of POMs is expected to find significant applications in biomaterials, if one considers the extensive use of PHEMA or PHEMA-based copolymers in biomaterial applications (such as contact lenses, implanting materials, etc.),⁴⁴ and in general, in many thermal curing processes in industry.

Conclusions

In the present paper, the capability of both Mo_{18}^{6-} and W_{18}^{6-} ions to thermally generate protons within PHEMA films is demonstrated. The acid is generated from the thermal reduction of POMs and the associated oxidation of a small percentage of PHEMA hydroxyl groups, and it subsequently catalyzes the cross-linking of PHEMA. The thermal reduction of POMs (within PHEMA films) is monitored with UV and FTIR spectroscopy, whereas from the kinetic study of that reaction the activation energy is estimated (62 kJ mol^{-1}). The thermally generated protons are detected by introducing a suitable acid indicator (MB) within POM-PHEMA films and monitoring the indicator's protonation with UV spectroscopy. From the combined FTIR and NMR study of PHEMA cross-linking within POM-PHEMA films, it was found that PHEMA cross-linking is an acid-catalyzed, ester breaking reaction (possibly transesterification), which is accompanied by a side reaction, the acid-catalyzed dehydration of PHEMA that leads to the formation of soluble (most likely cyclization) products. Finally, both POMs can be entirely removed from the thermally (e.g., at 140°C) cross-linked POM-PHEMA films upon incubation of the films in an aqueous solution of base (0.26 M TMAH), probably because of destruction of the POM structure by the base. From all the above, it is evident that both POMs investigated can be used for the thermal curing of polymer films containing hydroxyl groups (such as PHEMA).

Compared with common TAGs, both POMs have a considerable advantage: they can be entirely removed from the thermally cross-linked films through incubation of the films in an aqueous solution of base, expanding therefore, the field of their applications (e.g., biomaterials, fuel cells, and curing of coatings) to those that require the removal of TAG at the end of the process. Also, another difference of POMs in relation to common TAGs

(44) (a) Beek, M. V.; Jones, L.; Sheardown, H. *Biomaterials* **2008**, *29*, 780. (b) Giordano, C.; Causa, F.; Di Silvio, L.; Ambrosio, L. *J. Mater. Sci.: Mater. Med.* **2007**, *18*, 653. (c) Bertoluzza, A.; Monti, P.; Garcia-Ramos, J. V.; Simoni, R.; Caramazza, R.; Calzavara, A. *J. Mol. Struct.* **1986**, *143*, 469.

is that in the case of POMs, the acid generation results from an intermolecular thermal reaction between POM and polymer matrix, which starts only upon mixing the materials, whereas in common TAGs it usually arises from an intramolecular thermolysis reaction of TAGs. Finally, POMs can thermally yield protons, which are usually preferred in solid state catalysis, whereas a rather limited number of TAGs have been reported to act this way.

Supporting Information Available: UV monitoring of MB protonation caused by a known PAG (TPSHFA) and a solid acid ($\text{H}_3\text{PW}_{12}\text{O}_{40}$), FTIR study of PHEMA cross-linking by W_{18}^{6-} ions, NMR spectra of PHEMA and Mo_{18}^{6-} -PHEMA film, NMR study of PHEMA cross-linking by W_{18}^{6-} ions, removal of W_{18}^{6-} ions from thermally cross-linked W_{18}^{6-} -PHEMA films. This material is available free of charge via the Internet at <http://pubs.acs.org>.